

Document downloaded from:

<http://hdl.handle.net/10251/166749>

This paper must be cited as:

Ordóñez, J.; Martorell Alsina, SS.; Gallardo Bermell, S.; Ortiz Moragón, J. (2020). Monte Carlo model of a BEGe detector to support gamma-spectrometry in an emergency response. *Radiation Physics and Chemistry*. 172:1-7.  
<https://doi.org/10.1016/j.radphyschem.2020.108837>



The final publication is available at

<https://doi.org/10.1016/j.radphyschem.2020.108837>

Copyright Elsevier

Additional Information

# Monte Carlo model of a BEGe detector to support $\gamma$ -spectrometry in an emergency response

J. Ordóñez<sup>1</sup>, S. Martorell<sup>1,3</sup>, S. Gallardo<sup>2</sup>, J. Ortiz<sup>3</sup>

<sup>1</sup>Grupo de Medioambiente y Seguridad Industrial (MEDASEGI). Universitat Politècnica de València. Camí de Vera, s/n. 46022 València, Spain.

<sup>2</sup>Instituto Universitario de Seguridad Industrial, Radiofísica y Medioambiental (ISIRYM). Universitat Politècnica de València. Camí de Vera, s/n. 46022 València, Spain.

<sup>3</sup>Laboratorio de Radiactividad Ambiental. Universitat Politècnica de València. Camí de Vera, s/n. 46022 València, Spain.

**Abstract:** One of the problems of measuring high radioactivity in an emergency scenario is the fact that the detector can become saturated or reach a measuring dead time too high to give reliable results, which means repeating the measurement in different conditions with the associated delay in obtaining the results and the laboratory workers' risk of exposure. The counting rate can be controlled by varying the sample-to-detector distance as well as by using different source volumes. A Monte Carlo model of a BEGe detector was developed to analyse the system efficiency response for several measuring configurations (distances and volumes) using the MCNP6 code. The total efficiency curves were obtained for an energy range between 59.5 keV and 1836 keV. The simulations provided an estimation of the admissible  $\gamma$ -rate for different source volumes (in water matrix) and sample-to-detector distances to avoid detector saturation in given measurement conditions. The results were a compromise between geometry, distance and measuring time for certain emergency situations. Three case studies are provided to show the approach's effectiveness.

## 1. Introduction

Radiological threats due to nuclear or radiological accidents or radioactive attacks on society and the environment are increasingly perceived as a realistic possibility. There is also a broad consensus that the ability to efficiently identify such threats demands a sophisticated and dedicated infrastructure comprising specialised personnel, laboratories and advanced analytical instrumentation [Croudace et al., 2016].

An efficient approach to identifying such threats must be robust, fast, accurate and safe. Robust in the sense of always providing a reliable result, fast in terms of providing results in the shortest possible time, accurate in the characterization of all relevant radioisotopes within the radioactive material and safe in terms of reducing and controlling the risk of exposure to radiation of the laboratory personnel.

Simulation methods can be of great help in improving the approach to identify radiological threats [Maucec et al., 2004, Fantínová and Fojtík, 2014, Fonseca et al., 2017]. In this context, the Laboratorio de Radiactividad Ambiental (LRA) of the Universitat Politècnica de València (UPV, Spain) is developing  $\gamma$ -spectrometry procedures with semiconductor detectors to characterize high activity samples by a combination of experimental and simulation methods. These procedures are focused on the analysis of different measuring configurations to optimize the measurement sequence. To achieve accurate results a detailed characterization of the efficiency response of the system is mandatory and efficiency curves for the possible measuring configurations are also required. Computational techniques such as the Monte Carlo method can be useful to complement the experimental efficiency calibration procedure [García-Talavera et al., 2000, Hurtado et al., 2004, Dababneh et al., 2014, Ordóñez et al., 2019a] as they are able to simulate any case and obtain an efficiency map that considers all the possible combinations of source-to-detector distances and source volumes. Although the MCNP6 code was used in this work to simulate the efficiency calibration curves, different Monte Carlo codes such as FLUKA [Ferrari et al., 2005], PENELOPE [Salvat et al., 2003, Jurado-Vargas et al., 2006], GESPECOR [Sima et al., 2001], MCNP [Ródenas et al., 2000] or the GEANT4 toolkit [Agostinelli et al., 2003, Hurtado et al., 2004], among others, could be applied for the same purpose [Vidmar et al., 2008, Ordóñez et al., 2019b].

$\gamma$ -spectrometry detectors generally need a minimum interval of time to separate two independent events. This parameter, known as dead time, is mainly affected by the electronics associated with the detector system [Knoll, 2000]. In environmental laboratories under normal circumstances, the obtained dead time is usually low, but in emergencies, the activity of the sample may be so high that it significantly increases the measuring dead time, which in turn will lead to unreliable results. This parameter must therefore be taken into consideration before measuring an emergency response. The method used in this work is focused on not exceeding the maximum dead time value previously laid down by the laboratory.

This paper proposes an approach using an MCNP6 model of a BEGe detector to support  $\gamma$ -spectrometry in an emergency response that offers practical benefits and enhancements in rapid response and occupational safety in the context of nuclear and radiological emergencies. Three case studies are included to provide an insight into the approach.

## 2. Materials and Methods

### 2.1. Experimental set-up

The experimental set-up consisted of a gamma spectrometer with a BEGe-5030 (CANBERRA) detector calibrated to measure high activity samples and a multi-channel analyser with 8192 channels. The system has a relative efficiency of 40% at 1.33 MeV and a nominal resolution of 0.5 keV, 0.75 keV and 2.0 keV at 5.9 keV, 122 keV and 1332.5 keV, respectively. Table 1 describes the geometry features of the detector provided by the manufacturer.

**Table 1**  
Geometric features of the detector (manufacturer values)

Parameter	Nominal values
Ge crystal diameter	81mm
Ge crystal total length	30 mm
Front dead layer	0.4 $\mu$ m
Lateral/bottom dead layer	0.5 mm
Windows-to-detector distance	5.0 mm

Experimental measurements were made to calibrate the detector's efficiency and to validate the Monte Carlo model. The detector was calibrated for volumetric standard sources with different geometries, a 100 ml Petri box and a 5 ml cylindrical beaker. The samples contained a multi-gamma standard in a water matrix that consisted of  $^{241}\text{Am}$ ,  $^{109}\text{Cd}$ ,  $^{57}\text{Co}$ ,  $^{113}\text{Sn}$ ,  $^{137}\text{Cs}$ ,  $^{54}\text{Mn}$ ,  $^{88}\text{Y}$ ,  $^{65}\text{Zn}$ , and  $^{60}\text{Co}$  (from 59.54 keV to 1836.01 keV). Gamma-ray spectra were analysed on GENIE2000 Software [CANBERRA, 2009] and the efficiency ( $\epsilon$ ) of a given photon energy was obtained from the following expression:

$$\epsilon = \frac{N}{t \cdot A \cdot P_{\gamma}} \quad (1)$$

where N is the number of net counts in the peak, A is the source activity (Bq), t the counting time (s) and  $P_{\gamma}$  the photon emission probability. Validation was by comparing the simulated with the experimental Full Energy Peak Efficiencies (FEPE) through the simulated-to-experimental efficiency ratio with an acceptance range of  $\pm 5\%$  [0.95, 1.05].

Dead time is an important consideration in experimental measurements and in these particular cases had a value of around 0.6%, which was used as a reference in the screening approach adopted (Section 2.5).

### 2.2. Monte Carlo model

MCNP6 is a Monte Carlo transport code system for coupled neutrons, photons and electrons, with all the corresponding cross-section data to transport calculation. The F8 tally for photons and electrons was used to collect the deposited energy in the active crystal (Pulse Height Distribution, PHD) per emitted gamma particle. This tally provides the energy distribution of the pulses created in the active germanium crystal.

The data output was distributed into 8192 channels from 0 to 2040 keV simulating the multi-channel analyser used in the experimental set-up and considering the energy calibration obtained by GENIE2000 from the experimental measurements. A variance reduction method consisting of a cut-off for secondary particles with energies below 10 keV was applied. The number of histories in each simulation was established to achieve statistical errors lower than 1.5%.

The MCNP6 code was used to study the efficiency response of the system. Parameters such as the distance between the detector window and the germanium crystal, the dead layer thickness or the active crystal volume, among others, are of relevance in efficiency calibration and must be characterized [Ródenas et al., 2007, Blank et al., 2015, Chham et al., 2015, Jurado-Vargas et al., 2006]. The model proposed here (Fig. 1) was developed by optimizing these parameters and comparing the efficiency curves obtained through the simulations with the experimental data.

To characterize the detector's active volume, the electric response of the germanium crystal was analysed by the SALSA (Salamanca Lyso-based Scanning Array) method [Hernandez-Prieto et al., 2016]. This technique can estimate the dead layers around the crystal and reduce the uncertainties related to this parameter.

The detector model was validated by comparing the simulated efficiencies with experimental ones for the two different volumetric 5 ml and 100 ml samples placed at the top position (1 cm from the detector windows) and 5 cm higher.

Point sources of  $^{241}\text{Am}$ ,  $^{133}\text{Ba}$ ,  $^{137}\text{Cs}$  and  $^{60}\text{Co}$  placed at a height of 11 cm were used to complete the validation of the model.

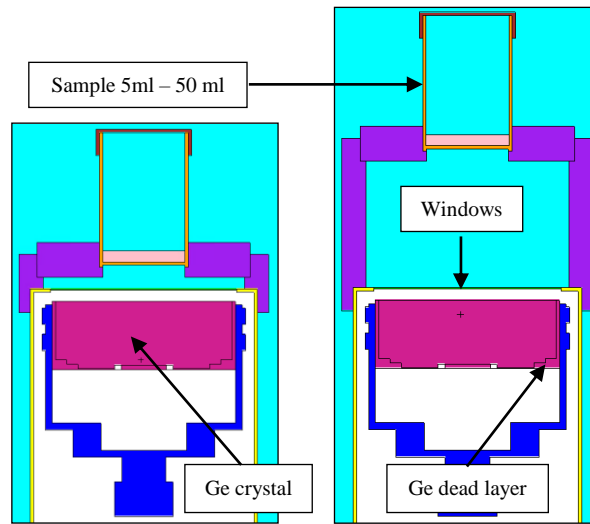


**Fig. 1.** BEGe-5030 detector model. Left: sample in top position (1 cm from the detector window). Right: sample 5 cm higher.

The simulated-to-experimental efficiency ratios were within the acceptance range [0.95, 1.05] in the energy range under study (Table 2 and Table 3).

**Table 2**

Simulated-to-experimental efficiency ratios (Uncertainty in brackets). Samples: 5 ml and 100 ml. Position: top and 6 cm.

Radionuclide	E (keV)	5 ml - Top	5 ml - 6 cm	100 ml - Top
<sup>241</sup> Am	59.54	1.00 (0.013)	0.98 (0.012)	1.00 (0.013)
<sup>109</sup> Cd	88.03	0.97 (0.029)	0.97 (0.029)	0.99 (0.030)
<sup>57</sup> Co	122.06	0.98 (0.014)	0.98 (0.014)	1.00 (0.014)
<sup>113</sup> Sn	391.69	0.95 (0.014)	0.97 (0.014)	0.99 (0.015)
<sup>137</sup> Cs	661.66	0.99 (0.023)	0.98 (0.023)	0.99 (0.023)
<sup>54</sup> Mn	834.83	0.99 (0.010)	0.98 (0.010)	0.98 (0.010)
<sup>88</sup> Y	898.02	1.02 (0.010)	0.97 (0.010)	1.03 (0.010)
<sup>65</sup> Zn	1115.52	0.99 (0.024)	0.98 (0.023)	1.00 (0.024)
<sup>60</sup> Co	1173.24	1.00 (0.005)	1.02 (0.005)	1.00 (0.005)
<sup>60</sup> Co	1332.50	1.01 (0.005)	1.02 (0.005)	1.02 (0.005)
<sup>88</sup> Y	1836.01	1.02 (0.008)	1.00 (0.008)	1.03 (0.008)

**Table 3.**

Simulated-to-experimental efficiency ratios (Uncertainty in brackets). Point sources. Position: 11 cm.

Radionuclide	E (keV)	Point source - 11 cm
<sup>241</sup> Am	59.54	0.99 (0.012)
<sup>133</sup> Ba	276.40	1.02 (0.014)
<sup>133</sup> Ba	302.85	1.01 (0.013)
<sup>133</sup> Ba	356.01	1.00 (0.014)
<sup>133</sup> Ba	383.85	1.00 (0.014)
<sup>137</sup> Cs	661.66	1.00 (0.021)
<sup>60</sup> Co	1173.24	1.01 (0.006)
<sup>60</sup> Co	1332.50	1.01 (0.006)

Different models were developed to cover all the possible measuring configurations of the proposed screening. A sample (cylindrical beaker used in the calibration, Fig. 1) with seven source volumes was modelled: 5 ml, 10 ml, 15 ml, 20 ml, 30 ml, 40 ml and 50 ml. All the samples were placed up to 20 cm from top geometry in steps of 2.5 cm.

### 2.3. Total Efficiency Curves

As the total efficiency curves of the different source volumes and source-to-detector distances were obtained, 63 efficiency curves were simulated. All the simulations considered an energy range from 59 keV to 1836 keV. Fig. 2 shows the total efficiency curves for the 5 ml sample. As expected, the closer the sample, the higher the efficiency in all the energy ranges. A large difference (~52%) was found between the top geometry and the one 2.5 cm higher. The source-to-detector distance effect on efficiency decreased with distance, being almost constant after a height of 10cm (91%-95%).

Something similar but smoother happened with the volume of the source (Fig. 3). The efficiency was found to decrease at higher source volumes as the mean distance between the source and the detector rose with volume.

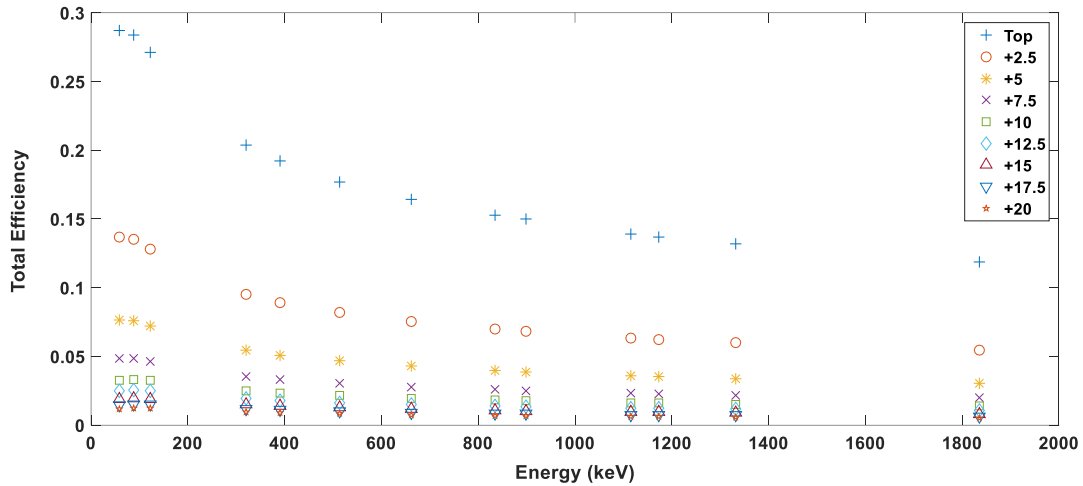


**Fig. 2.** Total efficiencies for different source-to-detector distances; Sample: 5ml

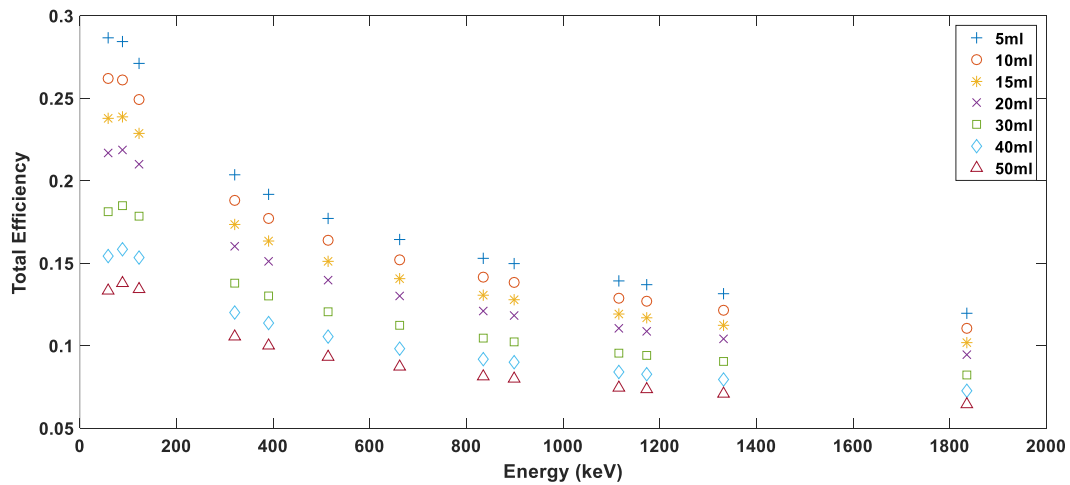


**Fig. 3.** Total efficiencies for different source volumes placed at the top geometry

### 2.4. Maximum $\gamma$ -rates

As commented in Section 2.1, a dead time of 0.6% was set in the experimental calibrations. The measuring configuration during the screening considers this value as a setting parameter. Knowing the resolving time of the detector (4  $\mu$ s), it is possible to calculate the maximum counting-rate (cps) that the system can process to meet the dead time criterion (~1500 cps). The measured counting-rate was highly affected by the  $\gamma$ -rate of the sample and the total efficiency of the system, which, in addition, depends on the measuring configuration, the energy of the gamma emission and the detector itself. In this frame, Monte Carlo simulations considering the mentioned parameters are required to characterize the total efficiency response of the system.

Table 4 shows the maximum values of the 5ml sample as a function of source-to-detector distance. As mentioned in Section 2.3, the top geometry has the highest total efficiencies and the lowest  $\gamma$ -rate values to meet the dead time criterion. On the other hand, this value increases with energy due to the loss of efficiency (Fig. 2).

Table 5 shows the equivalent results for the source volumes under study. The lowest values are those of the 5ml sample, since it had highest total efficiencies. Both analyses show also that  $^{241}\text{Am}$  would be the most restrictive

radionuclide with the lowest gamma energy (59.54 keV) and highest efficiency (Fig. 2 and Fig. 3). The comparison of the values for an energy of 59.54 keV in Table 5 shows that the maximum  $\gamma$ -rate for 50 ml is approximately twice that of 5 ml due to the loss of efficiency, but the activity in the sample would be 10 times higher. This means that if the dead time criterion is (hypothetically) satisfied for 5 ml placed in the top position, it may not be so for 50 ml. In such a case, the efficiency could be reduced by placing the sample higher.

**Table 4**

Screening table. Maximum allowed  $\gamma$ -rate ( $\gamma/s$ ) emitted by the sample to meet the dead time criterion; Sample: 5 ml

E (keV)	Top	+2.5 cm	+5 cm	+7.5 cm	+10 cm	+12.5 cm	+15 cm	+17.5 cm	+20 cm
<b>59.54</b>	5.26E+03	1.10E+04	1.97E+04	3.11E+04	4.60E+04	6.11E+04	8.06E+04	1.03E+05	1.29E+05
<b>88.04</b>	5.31E+03	1.12E+04	1.99E+04	3.11E+04	4.52E+04	5.93E+04	7.77E+04	9.89E+04	1.23E+05
<b>122.06</b>	5.57E+03	1.18E+04	2.09E+04	3.24E+04	4.64E+04	6.07E+04	7.92E+04	1.00E+05	1.25E+05
<b>320.08</b>	7.41E+03	1.59E+04	2.78E+04	4.26E+04	6.04E+04	7.84E+04	1.01E+05	1.28E+05	1.58E+05
<b>391.69</b>	7.87E+03	1.69E+04	2.96E+04	4.54E+04	6.44E+04	8.38E+04	1.08E+05	1.36E+05	1.68E+05
<b>513.99</b>	8.52E+03	1.84E+04	3.23E+04	4.96E+04	7.05E+04	9.18E+04	1.19E+05	1.49E+05	1.83E+05
<b>661.64</b>	9.19E+03	2.00E+04	3.51E+04	5.41E+04	7.68E+04	1.00E+05	1.30E+05	1.63E+05	2.00E+05
<b>834.83</b>	9.86E+03	2.16E+04	3.80E+04	5.86E+04	8.34E+04	1.09E+05	1.41E+05	1.78E+05	2.18E+05
<b>898.02</b>	1.01E+04	2.21E+04	3.90E+04	6.01E+04	8.56E+04	1.12E+05	1.45E+05	1.83E+05	2.24E+05
<b>1115.52</b>	1.09E+04	2.38E+04	4.20E+04	6.49E+04	9.26E+04	1.22E+05	1.58E+05	1.98E+05	2.43E+05
<b>1173.21</b>	1.10E+04	2.42E+04	4.27E+04	6.60E+04	9.44E+04	1.24E+05	1.60E+05	2.01E+05	2.47E+05
<b>1332.46</b>	1.15E+04	2.52E+04	4.45E+04	6.89E+04	9.85E+04	1.30E+05	1.68E+05	2.10E+05	2.58E+05
<b>1836.01</b>	1.26E+04	2.78E+04	4.92E+04	7.61E+04	1.09E+05	1.43E+05	1.85E+05	2.32E+05	2.84E+05

**Table 5**

Maximum allowed  $\gamma$ -rate ( $\gamma/s$ ) emitted by the sample to meet the dead time criterion; Position: Top geometry

E (keV)	5 ml	10 ml	15 ml	20 ml	30 ml	40 ml	50 ml
<b>59.54</b>	5.26E+03	5.77E+03	6.34E+03	6.97E+03	8.33E+03	9.79E+03	1.13E+04
<b>88.04</b>	5.31E+03	5.78E+03	6.32E+03	6.90E+03	8.17E+03	9.53E+03	1.09E+04
<b>122.06</b>	5.57E+03	6.05E+03	6.60E+03	7.19E+03	8.46E+03	9.83E+03	1.13E+04
<b>320.08</b>	7.41E+03	8.02E+03	8.70E+03	9.42E+03	1.10E+04	1.26E+04	1.43E+04
<b>391.69</b>	7.87E+03	8.51E+03	9.23E+03	9.99E+03	1.16E+04	1.33E+04	1.51E+04
<b>513.99</b>	8.52E+03	9.21E+03	9.98E+03	1.08E+04	1.25E+04	1.43E+04	1.62E+04
<b>661.64</b>	9.20E+03	9.93E+03	1.08E+04	1.16E+04	1.34E+04	1.54E+04	1.73E+04
<b>834.83</b>	9.86E+03	1.07E+04	1.15E+04	1.25E+04	1.44E+04	1.64E+04	1.85E+04
<b>898.02</b>	1.01E+04	1.09E+04	1.18E+04	1.28E+04	1.47E+04	1.68E+04	1.89E+04
<b>1115.52</b>	1.09E+04	1.17E+04	1.27E+04	1.37E+04	1.58E+04	1.80E+04	2.02E+04
<b>1173.21</b>	1.10E+04	1.19E+04	1.29E+04	1.39E+04	1.60E+04	1.83E+04	2.06E+04
<b>1332.46</b>	1.15E+04	1.24E+04	1.34E+04	1.45E+04	1.67E+04	1.90E+04	2.14E+04
<b>1836.01</b>	1.26E+04	1.37E+04	1.48E+04	1.60E+04	1.84E+04	2.09E+04	2.34E+04

## 2.5. Screening approach

The approach proposed here is based on the USEPA recommendations [EPA, 2008a]. Fig. 4 summarizes the methodology.

In the first stage, a 1L sample is sent to the laboratory with no information on its radionuclides or its activity. It is first tested with a contamination gamma-monitor to obtain the counting-rate (cps). As the monitor is calibrated for a sample geometry of 1L and energy of  $^{241}\text{Am}$  (59.54 keV) it can obtain an approximation of the  $\gamma$ -rate of the source and its activity, considering the gamma branching ratio for this emission. This radionuclide has the highest total efficiency of those considered in the experimental calibrations (Section 2.3) and is taken as reference at the beginning as being the most restrictive. In this step the sample is also classified either as an emergency or routine case. The next step is to take a small undiluted 5 ml sample and measure it for only 10 minutes in the detector in an emergency screening. The expected activity in the 5 ml sample can be determined from the 1L sample, as they are approximately proportional, considering their self-absorption in water. Before the preliminary measurement, the optimal source-to-detector distance is chosen to meet the dead time criterion, as explained in Section 2.4. The  $\gamma$ -rate in the 5 ml sample is compared to the values in Table 4 (for  $^{241}\text{Am}$ ) to select the best placement for the sample. However, it sometimes happens that the activity is so high that the sample cannot be placed far enough away from the detector to take the measurement (structural limitations). In this case, the sample should be diluted homogeneously with purified water to reduce the activity and begin again. A preliminary gamma spectrum is obtained after the screening. The analysis of the spectrum identifies the radionuclide with the biggest contribution to the overall  $\gamma$ -rate (preliminary report).

Finally, a measurement is carried out for 1h to completely characterize the sample (final report). Now the main radionuclide is known and the source volume can be raised to 50 ml. With the higher volume, the sample's activity rises in accordance with the counting-rate and improves the identification of other radionuclides. At this point, the optimal combination of volume and distance must be considered to optimize the counting-rate. The  $\gamma$ -rate that the sample would emit is compared to the maximum allowed for each combination of volume and distance, depending on the radionuclide/s identified in the screening (collection of tables such as Table 5 for different source-to-detector distances). As the higher the activity of the sample the higher the operators' dose exposure, the final configuration should also be taken considering the ALARA principle.

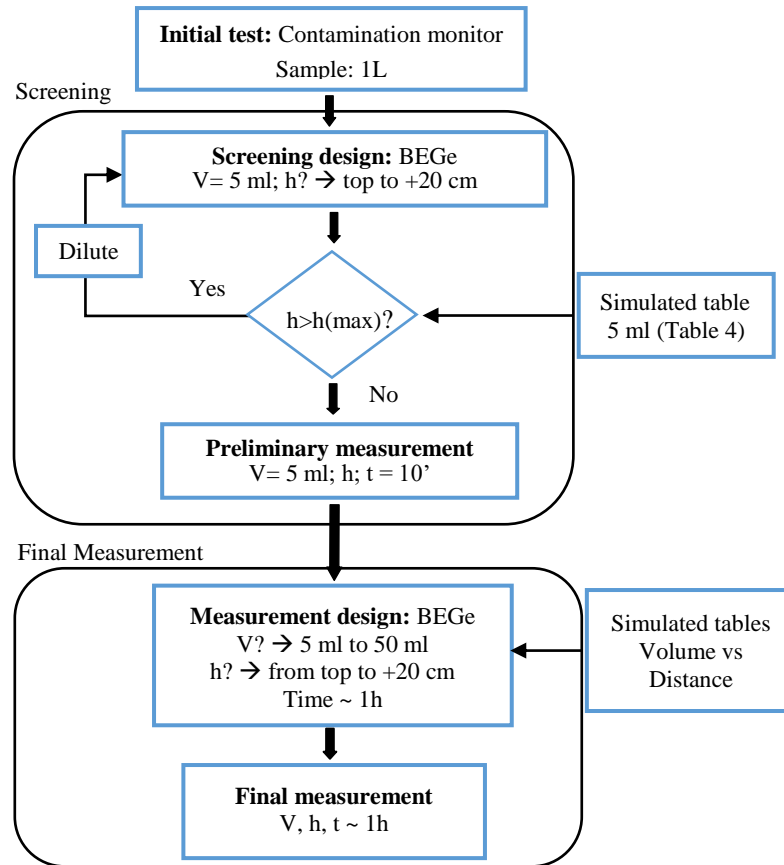


Fig. 4. Screening scheme

The problem is easier if only one radionuclide with only one main gamma-emission is considered. If after the preliminary measurement, for example,  $^{60}\text{Co}$  with a certain activity is detected as the main contributor with gamma emissions at 1173 keV and 1332 keV, both energies should be studied separately. Each one will have a different total efficiency and by considering the gamma branching ratio for each one it is possible to obtain the contribution of each emission to the total gamma-rate. Multiplying the gamma-rate of each emission obtained from the measured activity by its total efficiency, the counting-rate due to each one is obtained (Section 3.3 shows an example of a similar case). The total counting-rate (which cannot exceed the 1500 cps) is calculated as the sum of both. If more than one radionuclide is detected in the sample, a similar procedure is used, calculating the counting rate due to each one separately and adding them together.

The behaviour of the sample under different measurement conditions was simulated with a Monte Carlo model to support decision-making for the screening and measurement approach in Fig. 4 using the MCNP6 code [MCNP6TM Monte Carlo Team, 2013]. Total efficiencies were obtained (Fig. 2 and Fig. 3) and maximum  $\gamma$ -rate was calculated for the different configurations (see Table 4 (screening) and Table 5 (collection of tables for different source-to-detector distances)).

### 3. Application Cases

In this section three hypothetical cases are described to show the proposed approach's performance. All began with the 5 ml sample without any information on the radionuclides they contained. In the first two cases the main radionuclide in the sample was  $^{241}\text{Am}$  and  $^{137}\text{Cs}$ , respectively. The third consisted of a combination of both radionuclides. Similar results were obtained with the contamination monitor and the initial guess was  $^{241}\text{Am}$  to start the screening. The actual radionuclides in the sample were known after the preliminary measurement (screening).

#### 3.1. Case 1 ( $^{241}\text{Am}$ )

As there was no information available on the radionuclides present in the sample,  $^{241}\text{Am}$  was assumed to be the main radionuclide (most restrictive case). From the measurement of the 1L sample with the  $\gamma$ -monitor it was determined that the  $\gamma$ -rate in the 5 ml sample was  $6000\gamma/\text{s}$ . To decide the distance at which the sample must be placed (screening), this  $\gamma$ -rate must be compared with the maximum allowed for  $^{241}\text{Am}$ , using Table 4. The top position had a limit of  $5260\gamma/\text{s}$ , which was lower than the  $6000\gamma/\text{s}$  emitted by the sample. However, the sample could be placed 2.5 cm higher, with a limit of  $11000\gamma/\text{s}$ .



The gamma spectrometry measurement was carried out for 10 minutes at a position of +2.5 cm and the test determined that the main radionuclide present in the sample was indeed  $^{241}\text{Am}$ , measuring 18.10 kBq (corrected by the  $^{241}\text{Am}$  efficiency). Considering the branching ratio for the 59.54 keV gamma-emission (35.9%), 6500  $\gamma/\text{s}$  would be emitted by the source, slightly higher than the one predicted by the  $\gamma$ -monitor.

After the screening, the final measurement must be made for 1h. To improve the detection of other possible radionuclides with lower activity, a greater volume of source was required to increase the counting-rate and thus obtain better statistics. To decide the optimal configuration of volume and distance, Table 5 must be checked to compare the  $\gamma$ -rate in each sample with the maximum allowed. Table 6 lists the maximum allowable  $\gamma$ -rate for the possible configurations. The second column shows the  $\gamma$ -rate of each sample, which rises with volume. Green values are permitted combinations and red values are not. Orange values are acceptable although green are preferred from the statistical point of view.

**Table 6**

Maximum allowed  $\gamma$ -rate for each measuring combination ( $^{241}\text{Am}$ ). Green: allowed; Red: not allowed; Orange: allowed but with no interest

Sample	$\gamma$ -rate in the sample	Top	+2.5cm	+5cm	+7.5cm	+10cm
5ml	6.5E+03	5.26E+03	1.10E+04	1.97E+04	3.11E+04	4.60E+04
10ml	1.3E+04	5.77E+03	1.18E+04	2.08E+04	3.25E+04	4.69E+04
15ml	2.0E+04	6.34E+03	1.27E+04	2.22E+04	3.43E+04	4.92E+04
20ml	2.6E+04	6.97E+03	1.37E+04	2.37E+04	3.64E+04	5.19E+04
30ml	3.9E+04	8.33E+03	1.59E+04	2.70E+04	4.10E+04	5.80E+04
40ml	5.2E+04	9.79E+03	1.84E+04	3.07E+04	4.62E+04	6.49E+04
50ml	6.5E+04	1.13E+04	2.10E+04	3.46E+04	5.18E+04	7.24E+04

The best choice in terms of improving the measurement statistics will be the one whose  $\gamma$ -rate is below and closest to its limit. In this case, the configuration sample of 30 ml placed at 7.5 cm over the top position maximizes this parameter, with 3.9E+04  $\gamma/\text{s}$ , which represents 95% of the 4.1E+04  $\gamma/\text{s}$  limit. As the activity increases with volume, the final solution should also consider the dose exposure according to ALARA principle.

### 3.2. Case 2 ( $^{137}\text{Cs}$ )

This case began like Case 1 with 6000  $\gamma/\text{s}$  in the 5 ml sample. As previously, the sample was placed at 2.5 cm over the top position for the preliminary measurement. The measurement was carried out for 10 minutes and the result determined that the main radionuclide present in the sample was  $^{137}\text{Cs}$ . The sample activity was 7.18 kBq (corrected by the efficiency of the  $^{137}\text{Cs}$ ). Considering the branching ratio for the 661.7 keV gamma-emission (85%), 6100  $\gamma/\text{s}$  would be emitted by the source. The initial guess of 6000  $\gamma/\text{s}$  was determined with the  $\gamma$ -monitor assuming  $^{241}\text{Am}$ .

For the final measurement, as  $^{137}\text{Cs}$  has lower efficiency than  $^{241}\text{Am}$ , 0.6% of dead time could be satisfied in the top position. The homologous tables in Table 5 must be checked for the different source-to-detector distances under study. The possible new configurations are summarized in Table 7.

**Table 7**

Maximum allowed  $\gamma$ -rate for each measuring configuration ( $^{137}\text{Cs}$ ).

Sample	$\gamma$ -rate in the sample	Top	+2.5cm	+5cm	+7.5cm
5ml	6.10E+03	9.19E+03	2.00E+04	3.51E+04	5.41E+04
10ml	1.22E+04	9.93E+03	2.11E+04	3.65E+04	5.57E+04
15ml	1.83E+04	1.08E+04	2.23E+04	3.81E+04	5.78E+04
20ml	2.44E+04	1.16E+04	2.36E+04	4.00E+04	6.01E+04
30ml	3.66E+04	1.34E+04	2.65E+04	4.40E+04	6.52E+04
40ml	4.88E+04	1.54E+04	2.96E+04	4.83E+04	7.10E+04
50ml	6.10E+04	1.73E+04	3.28E+04	5.30E+04	7.71E+04

In this case, the optimal configuration would be the 30 ml sample placed in the +5 cm position (Table 7) with a  $\gamma$ -rate of 3.66E+04  $\gamma/\text{s}$  and a limit of 4.40E+04  $\gamma/\text{s}$  (83%).

### 3.3. Case 3 ( $^{241}\text{Am}$ and $^{137}\text{Cs}$ )

In the hypothetical case that both the  $^{241}\text{Am}$  and  $^{137}\text{Cs}$  radionuclides were present in the sample, the most conservative configuration would be the same as if there was only  $^{241}\text{Am}$  (Table 6) due to its higher total efficiency. For a better-estimated choice, the design of the final measurement lies in calculating the contribution of each radionuclide to the overall gamma emission, then the measured cps due to each radionuclide and finally the total cps (Eqs. 2 to 5).

$$\gamma_{Am-241} = \gamma_T \cdot P_{Am-241} \quad (2)$$



$$\gamma_{Cs-137} = \gamma_T \cdot P_{Cs-137} \quad (3)$$

$$CPS_{Am-241} = \gamma_{Am-241} \cdot Eff\_total_{Am-241} \quad (4)$$

$$CPS_{Cs-137} = \gamma_{Cs-137} \cdot Eff\_total_{Cs-137} \quad (5)$$

$$CPS_T = CPS_{Am-241} + CPS_{Cs-137} \quad (6)$$

where  $\gamma_X$  and  $\gamma_T$  are the gamma-rate of each radionuclide and the total, respectively,  $P_X$  represents the contribution (%) of each radionuclide to the overall gamma-emission and  $CPS_X$  and  $CPS_T$  are the counting-rate of each radionuclide and total..

The total counting-rate must not exceed the limit of 1500 cps. In this case, the screening (10 min. measurement with the 5ml sample) indicates a gamma-rate of 6500  $\gamma/s$  from both  $^{241}Am$  and  $^{137}Cs$ . Table 8 summarizes the best combinations for five different contributions of each radionuclide following the procedure introduced in Section 2.5 for more than one gamma-emission. All the combinations show a cps value slightly below the limit of 1500 cps.

**Table 8**

Best combination for each contribution fraction

$P_{Cs137}(\%)$	$P_{Am241}(\%)$	Height	Volume	cps
10	90	+7.5 cm	30 ml	1382
25	75	+5 cm	20 ml	1489
50	50	+ Top	5 ml	1465
75	25	+7.5 cm	50 ml	1428
90	10	+5 cm	30 ml	1423

#### 4. Conclusions

The UPV's environmental radioactivity laboratory (LRA) developed a  $\gamma$ -spectrometry procedure that includes an emergency screening approach using a BEGe detector supported by detector simulations performed on a Monte Carlo model (MCNP6) to characterize high activity samples.

The MCNP6 simulations provided estimates of the admissible sample activity at different energies, source volume and sample-to-detector distances to avoid detector saturation by meeting the dead time criterion. The optimal configuration (maximum volume and minimal distance) changes according to the relative contribution of each radionuclide to the overall activity. The optimal configuration leads to a compromise between volume, sample position and measuring time while also considering ALARA principle.

The proposed method is applicable to different radionuclides and gamma-emissions (within the energy range under study) for this BEGe detector configured to measure high activity samples. The screening approach based on the use of tables derived from the Monte Carlo detector model can determine whether the sample needs pre-treatment, e.g. dilution, and the optimal measurement configuration. In emergency scenarios the screening can reduce the lab response time as well as the risk of contamination and exposure to radiation of lab personnel.

This work was carried out in a collaboration project between the Universitat Politècnica de València (UPV) and the Valencian Agency for Security and Emergency. The method described aims to support  $\gamma$ -spectrometry in an emergency response and offers practical benefits and improvements in rapid response and occupational safety in the context of nuclear and radiological emergencies.

#### Acknowledgements

The authors gratefully acknowledge the Cátedra CSN-UPV Vicente Serradell, Spain as well as the Laboratorio de Radiactividad Ambiental (Universitat Politècnica de València), Spain, for the dedicated funding and resources for this research work under Grant No. FPI-2015-S2-1576. The authors are also grateful to the Valencia Agency for Security and Emergency and the Generalitat Valenciana for their support in the "*Convenio de colaboración entre la Agencia Valenciana de Seguridad y Respuesta a las Emergencias y la Universitat Politècnica de València para el Desarrollo del Plan de Vigilancia Radiológica en Emergencias*" under Grant No. S7042000, 2018.

#### References

- Agostinelli S. et al. (2003). Geant4-a simulation toolkit. Nucl. Instrum Methods Phys Res A, 506, 250-303.
- Blank, B., Souin, J., Ascher, P. et al., (2015). High-precision efficiency calibration of a high-purity co-axial germanium detector, Nucl. Instrum. Methods A, 776, 34-44.
- Canberra. (2009). Genie 2000 Spectrometry Software Customization Tools. Canberra Industries, Merdin.

- Chham, E. et al. 2015. Monte Carlo analysis of the influence of germanium dead layer thickness on the HPGe gamma detector experimental efficiency measured by use of extended sources. *Appl. Radiat. Isot.* 95, 30–35.
- Croudace, I. W., Warwick, P. E., Reading, D. G., Russell, B. C. (2016). Recent contributions to the rapid screening of radionuclides in emergency responses and nuclear forensics. *Trends Anal. Chem.*, 85 (part B), 120-129.
- Dababneh, Sael, Al-Nemri, Ektimal, Sharaf, Jamal. (2014). Application of Geant4 in routine close geometry gamma spectroscopy for environmental samples. *J. Environ. Radioact.* 134, 27-34.
- Fantínová, K., Fojtík, P. (2014). Monte Carlo simulation of the BEGe detector response function for *in vivo* measurements of  $^{241}\text{Am}$  in the skull. *Radiat. Phys. Chem.* 104, 345-350.
- Ferrari, A., Sala, P.R., Fassó, A., Ranft, J. (2005). FLUKA: a multiparticle transport code (version 2005), CERN-2005-10, INFN/ TC-05/11, SLAC-R-773. CERN, Geneva.
- Fonseca, T.C.F., Mendes, B.M., Hunt, J.G. (2017). Simulation of internal contamination screening with dose rate meters. *Radiat. Phys. Chem.* 140, 112-115.
- García-Talavera, M., Neder, H., Daza, M.J., Quintana, B. (2000). Towards a proper modeling of detector and source characteristics in Monte Carlo simulations. *Appl. Radiat. Isot.* 52, 777.
- Hurtado, S., García-León, M., García-Tenorio, R. (2004). GEANT4 code for simulation of a germanium gamma-ray detector and its application to efficiency calibration. *Nucl. Instr. and Meth. A* 518, 764–774.
- Hernandez-Prieto, A., Quintana, B., Martín, S., Domingo-Pardo, C. (2016). Study of accuracy in the position determination with SALSA, a  $\gamma$ -scanning system for the characterization of segmented HPGe detectors. *Nucl. Instr. and Meth. A* 823, 98-106.
- Jurado-Vargas, M., Guerra, A. (2006). Application of PENELOPE code to the efficiency calibration of coaxial germanium detectors. *Appl. Radiat. Isot.* 64, 1319–1322.
- Knoll, G. F. (2000). *Radiation Detection and Measurement, 3rd ed - Wiley*
- Maucec, M., de Meijer, R.J., Rigollet, C., Hendriks, P.H.G.M. (2004). Detection of radioactive particles offshore by  $\gamma$ -ray spectrometry Part I: Monte Carlo assessment of detection depth limits. *Nucl. Instr. and Meth. A* 525, 593-609.
- Monte Carlo team, MCNP6TM – User’s manual, Version 1.0, Los Alamos National Laboratory, LA-CP-13-00634, May 2013.
- Ordóñez, J., Gallardo, S., Ortiz, J., Martorell, S. (2019a). Coincidence summing correction factors for  $^{238}\text{U}$  and  $^{232}\text{Th}$  decay series using the Monte Carlo method, *Radiat. Phys. Chem.* 155, 244-247.
- Ordóñez, J., Gallardo, S., Ortiz, J., Martorell, S. (2019b). Intercomparison of full energy peak efficiency curves for an HPGe detector using MCNP6 and GEANT4, *Radiat. Phys. Chem.* 155, 248-251.
- Ródenas, J., Martinavarro, A., Rius, V. (2000). Validation of the MCNP code for the simulation of Ge-detector calibration. *Nucl. Instr. and Meth. A* 450, 88–97.
- Ródenas, J., Gallardo, S., Ballester, S., Primault, V., Ortiz, J. (2007). Application of the Monte Carlo method to the analysis of measurement geometries for the calibration of a HP Ge detector in an environmental radioactivity laboratory. *Nucl. Instrum. Methods Phys. Res. B.* 263, 144-148.
- Salvat, F., Fernández-Varea, J.M., Sempau, J., (2003). PENELOPE—A Code System for Monte Carlo Simulation of Electron and Photon Transport (OECD Nuclear Energy Agency, Issy-les-Moulineaux, France).
- Sima, O., Arnold, D., Dovlete, C. (2001). GESPECOR: A versatile tool in gamma-ray spectrometry. *J. Radioanal. Nucl. Chem.*, 248, 359-364.
- U.S. Environmental Protection Agency (EPA). (2008). Radiological Laboratory Sample Analysis Guide for Incidents of National Significance—Radionuclides in Water. Revision 0. Office of Air and Radiation, Washington, DC. EPA 402-R-07-007.
- Vidmar, T, Aubineau-Laniece, I, Anagnostakis, M J, Arnold, D, Brettner-Messler, R, Budjas, D, et al., 2008. An intercomparison of Monte Carlo codes used in gamma-ray spectrometry.. *Appl. Radiat. Isot.* 66 (6–7), 764–768.